frontiers | Frontiers in Earth Science

TYPE Original Research
PUBLISHED 27 January 2025
DOI 10.3389/feart.2024.1518390

OPEN ACCESS

EDITED BY
Dongliang Luo,
Chinese Academy of Sciences (CAS), China

REVIEWED BY
Alexandru Onaca,
West University of Timișoara, Romania
Mateo A. Martini,
National University of Cordoba, Argentina
Maciej Dąbski,
University of Warsaw, Poland

*CORRESPONDENCE
Ella Wood,
efw5@st-andrews.ac.uk

RECEIVED 28 October 2024
ACCEPTED 27 December 2024
PUBLISHED 27 January 2025

CITATION
Wood E, Bolch T and Streeter R (2025) Insights from feature tracking of optical satellite data for studying rock glacier kinematics in the Northern Tien Shan. *Front. Earth Sci.* 12:1518390. doi: 10.3389/feart.2024.1518390

Insights from feature tracking of optical satellite data for studying rock glacier kinematics in the Northern Tien Shan

Ella Wood[1,2]*, Tobias Bolch[3,4] and Richard Streeter[1]

[1]School of Geography and Sustainable Development, University of St Andrews, St Andrews, United Kingdom, [2]Department of Geography, University of Bonn, Bonn, Germany, [3]Institute of Geodesy, Graz University of Technology, Graz, Austria, [4]Central-Asian Regional Glaciological Centre of Category 2 Under the Auspices of UNESCO, Almaty, Kazakhstan

Rock glaciers are prevalent across the Tien Shan and exhibit complex, but poorly understood kinematics linked to climate and environmental fluctuations. This study employed a frequency domain cross-correlation method to investigate rock glacier velocities in the Northern Tien Shan. We compared different sources of satellite imagery, including 0.5m Pléiades, 3m Planet, 10m Sentinel-2 and 15m Landsat-8 data. Analysis of high-resolution Pléiades imagery in the Central Ile Alatau showed considerable spatial heterogeneity in flow. The highest median velocity of 0.65 m/yr was observed on Timofeyeva rock glacier, with an upper quartile value of 0.90 m/yr. Ordzhonikidze and Morennyi rock glaciers also exhibited high activity, with upper quartile values of 1.91 m/yr and 0.96 m/yr, respectively, despite considerably lower mean and median values than Timofeyeva. We observed bimodal velocity distributions on a number of rock glaciers, highlighting the limitations of using mean and median statistics for characterising rock glacier activity. Sentinel-2 data was capable of detecting kinematic patterns that closely reflected those identified by high-resolution Pléiades data. Velocities were derived from Sentinel-2 imagery for 672 rock glaciers across the Northern Tien Shan over a 7-year period (2016–2023). Many of the larger rock glaciers in the regional inventory exhibited active areas with velocities that exceeded 2 m per year. Topographic analysis in the Central Ile Alatau and visual inspection showed the fastest velocities to generally occur on lower, flatter areas near the rock glacier front. However, topography did not entirely explain the spatial flow heterogeneity. We interpret that these spatial patterns in activity are related to individual rock glacier's internal structure.

KEYWORDS

rock glacier, feature tracking, Tien Shan, kinematics, remote sensing, Central Asia

1 Introduction

Rock glaciers are common features of the mountain cryosphere. Whilst definitions of rock glaciers have long been debated, they are broadly described as landforms composed of an ice-debris mixture that exhibit signs of current or past flow downslope and exist under permafrost conditions (Berthling, 2011; Janke and Bolch, 2021; RGIK, 2023). Flow is a fundamental characteristic of rock glaciers and is closely intertwined with their ice-debris composition, morphology and relationship with climate. The

conglomerate nature of this ice-debris material makes rock glaciers heterogenous in terms of their morphological and flow characteristics, presenting many challenges to understanding the processes taking place. Rock glaciers play a role in cryospheric water storage, mountain hazards and landscape evolution. Research highlights rock glaciers as potentially hydrologically significant (Bolch and Marchenko, 2009; Azócar and Brenning, 2010; Jones et al., 2019; Jones et al., 2021; Halla et al., 2021) and an important part of the mountain debris transport system (Schrott, 1996; Barsch and Jakob, 1998).

The mountain cryosphere in Central Asia is a critically important hydrological resource (Bolch and Marchenko, 2009; Immerzeel and Bierkens, 2012; Shahgedanova et al., 2020). Water stored in glacier ice, snow, permafrost and rock glaciers in the Tien Shan is necessary to maintain river flow (Shahgedanova et al., 2018) and compensates for low summer precipitation on the Steppe (Bolch and Marchenko, 2009; Sorg et al., 2012; Bolch, 2017). Glacier mass loss has been widely observed across the Tien Shan in response to recent climate changes (Bolch, 2007; Niederer et al., 2008; Sorg et al., 2012; Farinotti et al., 2015; Pieczonka and Bolch, 2015; Zhang et al., 2022). There are concerns that "peak water" has already been reached in some catchments in the Tien Shan, with declining glacial runoff to be expected in the future (Shahgedanova et al., 2020). However, neither the climate response, hydrological significance nor the role of rock glaciers in landscape evolution and deglaciating mountain environments are well understood.

Research into flow dynamics is integral for understanding rock glaciers. Early literature assumed rock glaciers to have a constant flow state (Wahrhaftig and Cox, 1959), however seasonal, interannual and longer variations in flow have since been identified (Delaloye et al., 2010; Wirz et al., 2016; Kellerer-Pirklbauer et al., 2024). Rock glaciers are also shown to be accelerating in response to recent climate changes in the European Alps (Kellerer-Pirklbauer et al., 2017; Marcer et al., 2021; Thibert and Bodin, 2022; Kellerer-Pirklbauer et al., 2024). Similar tendencies were found in North America (Kääb and Røste, 2024) and for selected rock glaciers in Northern Tien Shan (Kääb et al., 2021). Optical feature tracking methods are well established for investigating flow dynamics within the field of glaciology (Scambos et al., 1992; Heid and Kääb, 2012; Dehecq et al., 2019; Millan et al., 2022), however, applying feature tracking to rock glaciers presents additional challenges. The relatively slow magnitude of rock glacier displacement, their situation on steep slopes and signals from other slope processes all present difficulties in determining clear velocity information (Scambos et al., 1992; Heid and Kääb, 2012; Dehecq et al., 2019; Millan et al., 2022).

Radar data is increasingly used to measure rock glacier flow using speckle tracking of high-resolution synthetic aperture radar (SAR) data or differential SAR interferometry techniques (DInSAR). DInSAR techniques can be used to identify displacements in the line of sight of the sensor with millimetre scale accuracy (Strozzi et al., 2020) and are unaffected by visibility limitations (Villarroel et al., 2018). Studies have applied DInSAR techniques to investigate rock glacier velocities across the globe (Lilleoren et al., 2013; Liu et al., 2013; Barboux et al., 2014; Strozzi et al., 2020; Kääb et al., 2021; Bertone et al., 2022). However, optical feature tracking methods can provide information on flow direction as well as velocity magnitude and often have a higher spatial resolution than radar data. This makes them suited to resolving heterogenous flow dynamics, particularly on landforms that exhibit a wider range of velocities. Furthermore, optical data is often available for a longer time-period; feature tracking techniques don't suffer from decorrelation issues associated with faster flow and are not limited by orientation, compared to SAR data. Both optical and radar approaches for investigating rock glacier velocities are valuable and can be used in conjunction with one another (Necsoiu et al., 2016; Kääb et al., 2021).

Rock glaciers are prevalent across the Tien Shan as the semi-arid mountain environment provides favourable conditions for their formation (Gorbunov and Titkov, 1989; Gorbunov et al., 1992; Blöthe et al., 2019; Bolch et al., 2019). The best investigated ranges of the Tien Shan are the Ile Alatau and Kungöy Alatau, here 871 rock glaciers have been identified from aerial imagery, covering an area of more than 90 km^2 (Titkov, 1988; Gorbunov et al., 1998). Gorbunov et al. (1992) manually measure rock glacier displacement from aerial images. Velocity detection from high resolution optical imagery is also utilised by Sorg et al. (2015), Bolch and Strel (2018), and Kääb et al. (2021). Sorg et al. (2015) combine optical remote sensing with tree ring data to establish a long-term record of flow for four rock glaciers across the Kyrgyz and Kazakh Tien Shan. SAR interferometric methods are used to establish regional velocity inventories by Wang et al. (2017), Kaldybayev et al. (2023) and Kääb et al. (2021) who use a combined approach. These studies show rock glaciers in the Tien Shan to be relatively fast flowing but with considerable variability between landforms. Velocities have increased in this region since the 1960s/1970s (Gorbunov et al., 1992; Kääb et al., 2021), reflecting similar observations on rock glaciers in the European Alps. Temporal variations in flow activity, fluctuating at varying timescales, have been observed (Sorg et al., 2015; Kääb et al., 2021), sometimes exhibiting pulse-like flow regimes (Gorbunov et al., 1992).

This study aims to 1) test and apply a feature tracking method implemented in Python; 2) compare different sources of optical imagery and their application for investigating rock glacier kinematics at different spatial scales; 3) evaluate the spatial patterns of activity, particularly at the sub-landform scale and consider the possible drivers of this heterogeneity. We look at how feature tracking methods can be adapted to the context of rock glaciers and present a processing workflow using frequency domain cross-correlation that can be implemented in Python. We then compare the results from different sources of optical imagery with different spatial resolutions. High-resolution velocities are derived for the Central Ile Alatau using 0.5 m Pléiades data and 10 m resolution Sentinel-2 data is used to derive velocities across the whole Northern Tien Shan. We investigate the relationships between surface velocity and topography using high resolution data from rock glaciers in the Central Ile Alatau, to better understand the drivers of spatial flow heterogeneity.

2 Study area

This research focuses on the Northern Tien Shan, which is host to many large, fast flowing rock glaciers (Kääb et al., 2021). The Northern Tien Shan encompasses the mountain ranges between Issyk-Kul Lake in the south and the Kazakh Steppe to the north (Figure 1). This includes the Ile Alatau and Kungöy

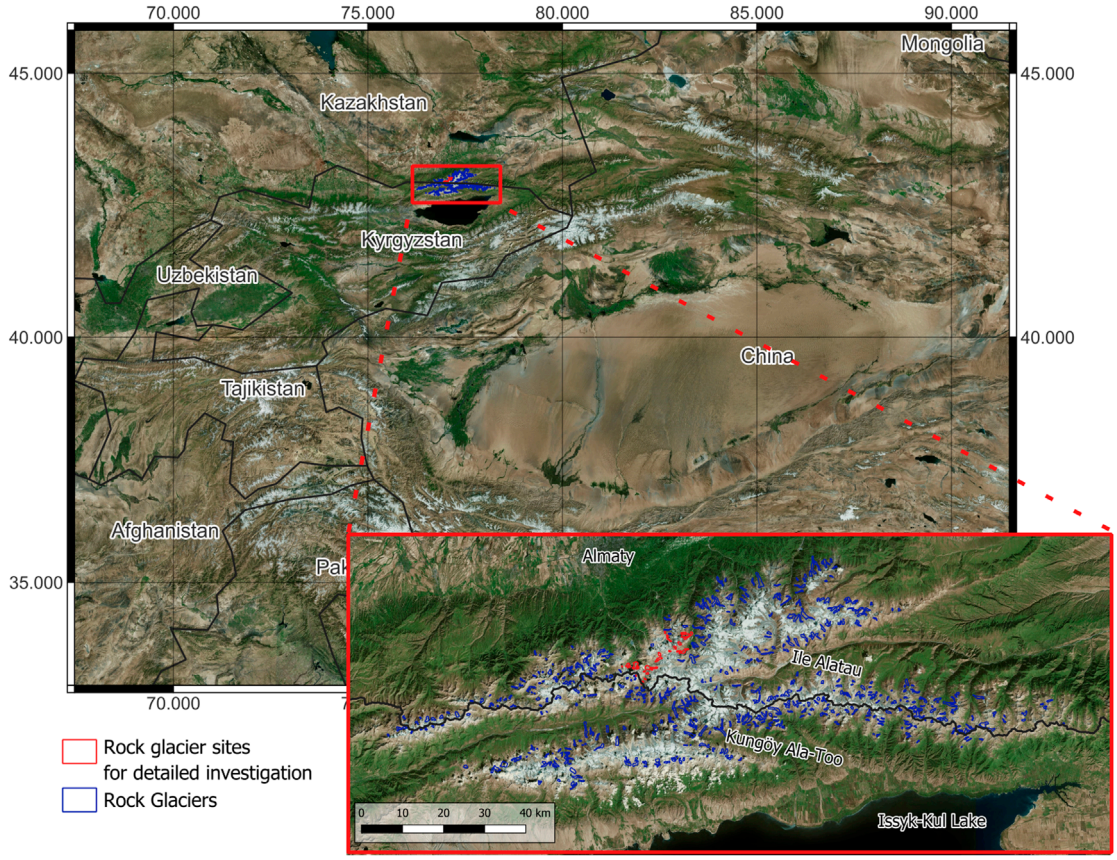

FIGURE 1
Study area showing the Northern Tien Shan region subdivided into the Ila Alatau and Kungöy Ala-Too mountain ranges. Rock glacier outlines were produced by this study and the base map is from Bing imagery.

Ala-Too ranges (formerly Zailijskij and Kungej Alatau) along the border of Kazakhstan and Kyrgyzstan (Figure 1). Peak Talgar marks the highest point in the region with an elevation just under 5000 m. The mountain range is uplifting and is subject to frequent tectonic activity, which has been known to trigger mass movements (Yadav and Kulieshius, 1992; Havenith et al., 2015). The geology is mainly Devonian, Silurian and Carboniferous age Granites, with some Cambrian gneisses in the Kungöj Ala-Too (Bolch and Gorbunov, 2014). There is a strong seasonality in temperature and precipitation with precipitation maxima in early summer June-July in the mountains (Shahgedanova et al., 2020). Temperatures in the Tien Shan have risen since the 1950s, with warming rates that exceed the global average (Bolch, 2007; Bolch and Marchenko, 2009); precipitation has also been found to increasingly fall as rain instead of snow (Chen et al., 2016).

3 Materials and methods

3.1 Rock glacier outlines and classification

We updated and extended the existing rock glacier inventory by Kääb et al. (2021) to cover the whole Ile and Kungöy Alatau of Northern Tien Shan. Mapping of the rock glacier outlines was done by process of manual identification and delineation based on visual morphology from Bing and Google Earth Basemap imagery. The delineation method followed the principals from the International Permafrost Association guidelines on Rock Glacier Inventories and Kinematics, RGIK (RGIK, 2023). We used existing outlines from Kääb et al. (2021) and Bertone et al. (2022) as a starting point for the inventory. Non-rock glacier landforms identified by Kääb et al. (2021) were excluded, as movements relating to solifluction, permafrost subsistence and other debris movements were included in the previous inventory. We then mapped an additional 290 rock glaciers at the eastern and western edges of the mountain ranges. Many outlines were further refined based on visual inspection and polygons inaccurately splitting up singular rock glaciers were merged.

We conducted more detailed analyses of 17 rock glaciers in the Central Ile Alatau. These landforms were selected due to their coverage by high resolution Pléiades imagery (Figure 2) and information from previous research. Four rock glaciers covered by the Pléiades imagery were excluded from the results due to snow and shadow cover. Multipart rock glaciers were subdivided into their morphological units for analysis, the rock glaciers were numbered, and individual sub-units indicated by a letter, e.g., 10A (Figure 2). The rock glaciers represented a range of rock glacier types, with different upslope connections including talus-supplied

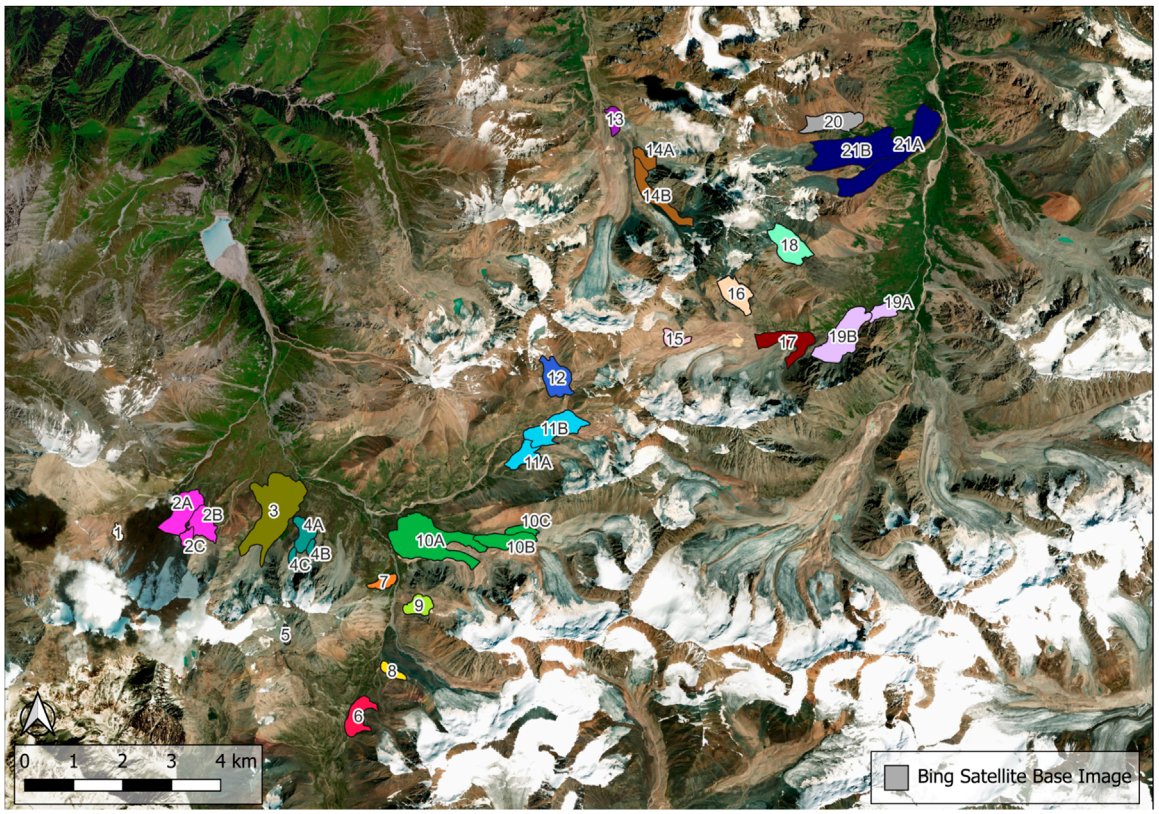

FIGURE 2
Rock glaciers in the Ulken Almaty, Kishi Almaty and Sol Talgar valleys, which are the subject of detailed analyses (outlines marked in red in Figure 1), map central coordinate is 43.02N, 77.08E. Colour coding indicates rock glacier ID (see supplementary material) and is used throughout the paper.

landforms, glacier connected landforms, glacier forefield-connected landforms and poly-connected landforms. The upslope connection was recorded for these rock glacier units based on the RGIK guidelines (RGIK, 2023).

3.2 Satellite data

This study compared different sources of satellite derived optical imagery with different spatial resolutions. We compared 0.5 m resolution Pléiades, 3 m Planet, open-source 10 m Sentinel-2 MSI and 15 m panchromatic Landsat-8 OLI data (Table 1). The images were selected based on cloud and snow free acquisitions collected between late June to mid-September. We aimed to find clear images with the closest acquisition day and month in their respective years. However, the limited number of suitable images due to variations in cloud cover meant that the offsets ranged between 4 and 37 days (Table 1), over the 7-year time period these differences were considered minor. The feature tracking was run on either the green or the panchromatic band; individual bands were extracted from multiband images during the pre-processing (Figure 3). A series of test runs found the green band to be the most effective for Planet and Sentinel imagery, as it resulted in the highest number of successful matches compared to other visible or NIR bands. The panchromatic band was used for the Pléiades and Landsat imagery due to the higher resolution compared the visible and NIR bands. Pléiades ortho images were produced from stereo data collected in 2016 and 2020 and processed according to Bhattacharya et al. (2021). The Pléiades imagery was used to conduct detailed analyses on the rock glacier complexes in the Central Ile Alatau. Planet, Sentinel-2 and Landsat image pairs had a 7-year time step and were acquired in late summer in 2016 and 2023. Sentinel-2 imagery was used for the regional scale analysis.

3.3 Feature tracking method

A number of different feature tracking algorithms have been utilised by previous studies including COSI-Corr (Necsoiu et al., 2016; Hassan et al., 2021) CIAS (Kääb and Vollmer, 2000; Strozzi et al., 2004; Kääb et al., 2007; Kääb et al., 2021) Environmental Motion Tracking (EMT) (Groh and Blöthe, 2019; Blöthe et al., 2021), IMCORR (Cusicanqui et al., 2021) and IMGRAFT (Monnier and Kinnard, 2017) to study rock glacier flow. These approaches are all based on similar principles but vary in terms of the steps they include, the degree of parameter flexibility, their accessibility and their user friendliness. Here we opted to use an intensity based cross-correlation technique implemented in Python, using the Arosics package, to conduct the image cross-correlation (Scheffler et al., 2017). Intensity-based matching methods work

TABLE 1 Sources of optical imagery used for feature tracking with image acquisition dates, image resolution, image band used and region.

Image source	Collection date	Resolution	Band used	Coverage
Pléiades	27/08/2016	0.5 m	Panchromatic	Big and Small Almaty and Left Talgar Valleys
Pléiades	16/09/2020	0.5 m	Panchromatic	Big and Small Almaty and Left Talgar Valleys
Planet	07/09/2016	3 m	Green Band	Big and Small Almaty and Left Talgar Valleys
Planet	03/09/2023	3 m	Green Band	Big and Small Almaty and Left Talgar Valleys
Sentinel 2A	09/08/2016	10 m	Green Band	N. Tien Shan, western half
Sentinel 2A	15/09/2026	10 m	Green Band	N. Tien Shan, western half
Sentinel 2A	24/07/2023	10 m	Green Band	N. Tien Shan, eastern half
Sentinel 2A	30/08/2023	10 m	Green Band	N. Tien Shan, eastern half
Landsat Pan	15/09/2016	15 m	Panchromatic	Big and Small Almaty and Left Talgar Valleys
Landsat Pan	03/09/2023	15 m	Panchromatic	Big and Small Almaty and Left Talgar Valleys

in the frequency domain by observing the spectral signature of grey values in a given area and identifying the same signature within a larger search window in the subsequent images (Gruen, 2012). The cross-correlation method used here, from Arosics, uses frequency domain normalised cross-correlation, designed to be robust when working with data from multiple sensors and timescales (Scheffler et al., 2017). We found Arosics suited to comparing different sources of imagery and working with sub-optimal image pairs with differences in illumination level, snow and light cloud cover. Arosics' primary function is for image co-registration, and it had not previously been applied to rock glacier velocities. We developed a processing chain that integrated the pre and post processing steps (Figure 3).

Pre-processing increased the number of accurate matches detected by the feature tracking, whilst post processing was necessary to remove erroneous matches and ensure a more accurate final output. A major problem when investigating the velocities of slow-moving landforms is inaccurate image co-registration, which can lead to flow vectors being obscured or distorted. Co-registration errors were corrected for by conducting initial co-registration of the images based on stable ground areas. We found co-registration errors across all types of imagery. The 2016 Pléiades image was shifted −2.18/-0.08 m to correct for co-registration errors (Figure 4). For the high-resolution analyses, stable ground areas were manually selected close to the rock glaciers within the Central Ile Alatau whilst during the regional analysis co-registration was conducted on the urban area of Almaty. This was because co-registration of the lower resolution, regional imagery worked best on larger areas of flat terrain with clearly distinguishable features such as buildings. In the absence of any ground control points the most recent image was assumed to be the most accurate.

Initial tests were run on small areas without masking to check the displacement on the rock glaciers relative to the surrounding terrain, as shown in Figure 4. However, for all other analyses masks were applied to limit noise in the data and reduce the processing time. For the high-resolution data, the rock glacier outlines were used as a mask to exclude all surroundings, which reduced the processing time. When conducting the regional analyses, feature tracking was run across smaller sub-regions encompassing both the rock glaciers and the surrounding terrain. Here we applied a combined snow and cloud cover mask based on a Normalised Difference Snow Index to reduce noise in the output. The difference in approach taken was because the lower resolution of the regional analysis meant that using a targeted rock glacier mask distorted the results along the rock glacier edges. The velocity map was later clipped to the rock glacier outlines. The images were normalised and resampled during the pre-processing to facilitate better comparison; these steps can be omitted from the workflow (Figure 3) if not necessary.

A series of neighbourhood filters (Figure 3) for velocity magnitude and vector direction were applied based on the method used by Kääb et al. (2021). Data points were compared to the mean value of their neighbouring pixels and removed if the difference is greater than a set threshold. Here, the threshold for the directional neighbourhood filter was set at 90° and a 3-meter threshold applied for the magnitude neighbourhood filter. A further overall magnitude filter was applied as a percentage of the overall distribution of velocity values, this was set at 99.5%, except for the analysis of the Pléiades data where this filter was excluded. The results were interpolated to neighbouring no data pixels within a certain radius and averaged into meters per year.

We used the lower limit of detection as an indicator of overall uncertainty, as we considered this the greatest source of uncertainty. The lower limit of detection was assumed to be equivalent to the mean offset on areas of stable ground. Feature tracking was conducted on stable ground for all sources of imagery. Stable ground areas were manually delineated in the Ulken Almaty Valley, independent of those used for co-registration but kept consistent across the different imagery. The mean velocity magnitude on

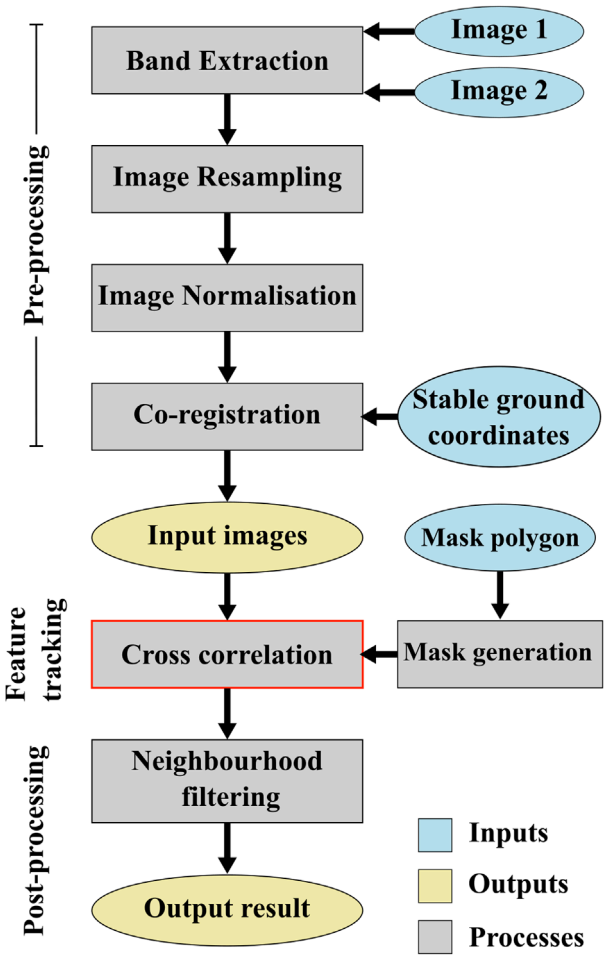

FIGURE 3
Feature tracking processing workflow, including inputs, pre-processing steps, main cross-correlation (outlined in red), post processing and final output.

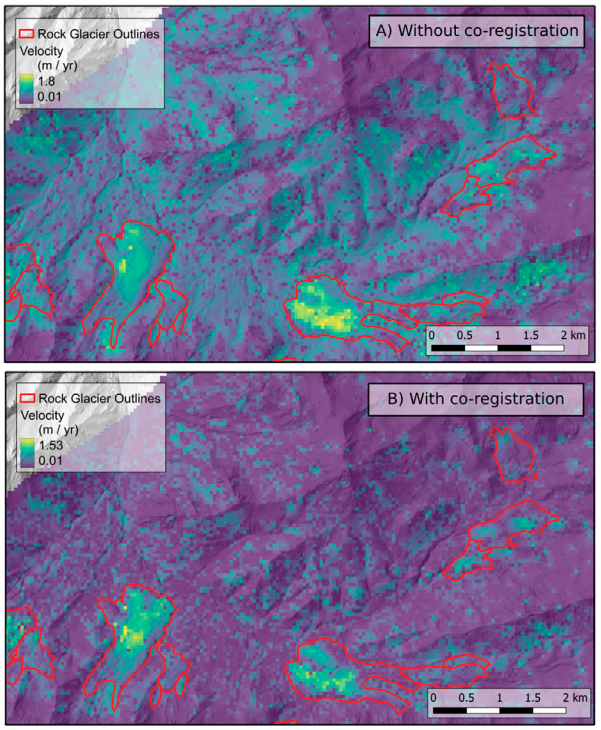

FIGURE 4
Results of feature tracking **(A)** with and **(B)** without co-registration, showing removal of background noise.

the stable ground areas was taken to be the lower limit of detection (Table 2).

3.4 Topographic analysis

Topographic analysis was conducted using the 2 m digital elevation model (DEM) generated from the 2016 Pléiades image. We compared rock glacier surface slope, velocity magnitude, flow direction and local surface aspect. Slope and aspect maps were derived at a 10 m resolution, matching the resolution of the velocity results. Mean slope, aspect and velocity were calculated for each rock glacier sub-unit and compared statistically. Then for the sub-landform scale analysis the corresponding flow and topographic parameters were extracted for each 10 m pixel. Profiles of velocity magnitude and elevation were extracted along transects manually mapped along the flow centrelines. Spearman's or Pearsons rank tests for correlation were used to investigate the relationships between velocity magnitude and slope based on the distribution of the data. Circular tests for correlation were used for the analyses between aspect and flow direction. Results with P-values of <0.05 were considered statistically significant (Table 3). Shuttle Radar Topography Mission (SRTM) data was used to derive rock glacier elevations in the regional inventory.

4 Results

4.1 Comparison of different sources of optical imagery

Pléiades, Planet, Sentinel-2 and Landsat-8 imagery were all capable of identifying some level of rock glacier displacement (Figure 5). As expected, the Pléiades imagery produced the most detailed results and was used as a baseline for comparison of the other sensors. Sentinel-2 and Landsat-8 imagery were also capable of detecting sub-landform scale spatial patterns of flow that generally corresponded to the results derived from the Pléiades data. The Planet data struggled to detect coherent flow fields and produced more binary outputs with areas of faster flow and areas of very limited displacement.

The spatial pattern detected by the Sentinel data showed the strongest resemblance to the Pléiades data out of the sensors investigated. The notable outlier was on the "thumb" lobe on the north-western edge of Morennyi (see Figure 5). Here Pléiades detected a fast lobe of flow on the north-western 'thumb' of the rock glacier which was not picked up by the Sentinel-2, Planet or Landsat-8 imagery. This discrepancy was also partly

TABLE 2 Offset on stable ground used for uncertainty estimates.

	Mean stable ground offset (m/yr)	Standard deviation (m/yr)	Spatial resolution (m)
Pléiades	0.21	0.12	0.5
Planet	0.15	0.04	3
Sentinel	0.35	0.10	10
Landsat	0.40	0.11	15

responsible for the difference in maximum velocities between the scenes, the maximum velocity detected on Pléiades was 2.28 m/yr compared to 1.29 m/yr for the Sentinel imagery and 1.19 m/yr for Landsat (Figure 5). However, Landsat and Sentinel imagery both performed well otherwise. Compared to the Landsat-8 data, the higher resolution of Sentinel-2 increased the spatial resolution of the final results achievable and slightly reduced the uncertainty. Based on these findings we used Sentinel-2 data for the regional scale analysis.

4.2 High-resolution kinematics in the Central Ile Alatau from Pléiades imagery

The velocities of the 17 rock glacier complexes investigated ranged from <0.1 m/yr to just under 2.5 m/yr for the period 2016–2020 (Figure 6), with an uncertainty of 0.21 m/yr. The rock glaciers showed strong spatial heterogeneity with clear inter and intra landform variation in velocities, often with faster streams related to morphological lobes of flow. Activity also varied between different units of rock glacier complexes, with the fastest velocities generally found on the lower lobe close to the rock glacier terminus. The fastest median velocity of 0.65 m/yr was exhibited on the main body of Timofeyeva rock glacier. However, Ordzhonikidze A and Morennyi exhibited the most prominent areas of high activity (Figure 6) and had the highest upper quartile velocity values (Table 3; Figure 7).

Velocity magnitude was sampled at 10 m resolution and plotted to show the distribution of velocity values for each rock glacier unit (Figure 7). Timofeyeva A exhibited the highest median velocity of 0.65 m/yr, with an upper quartile value of 0.90 m/yr. Ordzhonikidze and Morennyi rock glaciers also exhibited high activity, with upper quartile values of 1.91 m/yr and 0.96 m/yr respectively, despite having lower mean and median values than Timofeyeva (Figure 7; Table 3). Several of the rock glaciers exhibited a bimodal distribution of velocity values (Figure 7), with clear areas of high activity and areas of relative inactivity within the same landform. This pattern was particularly distinctive on Timofeyeva A, Gorodetsky A and Ordzhonikidze A. Furthermore, we observed considerable differences between mean and median values (Table 3).

4.3 Relationships between surface velocity and local topography

Rock glaciers with South-Westerly or North-Easterly orientations tended to exhibit faster flow compared to those with North-Westerly or South-Easterly aspects (Figure 8A). Of the nine rock glaciers with mean velocities exceeding 0.5 m/yr, all were located in the SW or NE quadrants expect for Gorodetsky A (10A) which had a WNW orientation. Figure 8A shows a cluster of noticeably faster flowing and larger rock glaciers in the North-East quadrant. At an inter landform scale there was no significant relationship between mean slope and mean velocity (Figure 8B). However, analysis at the individual landform level showed many rock glaciers to have a significant negative relationship between slope and velocity, with values sampled at a 10 m resolution (Table 3). This relationship was strongest on the main body of Archaly rock glacier. This supports visual observations that the fastest velocities tended to be located near the rock glacier termini where compressive stresses cause the rock glacier body to thicken and the surface to flatten out, see discussion for more details. However, at the sub-landform scale nine rock glacier units showed no significant relationship between slope and velocity and four exhibited a positive relationship. There were no clear differences in topographic–velocity relationships relating to the rock glacier upslope connection (Table 3); however, the sample was dominated by glacier-connected or glacier-forefield-connected type rock glaciers.

A closer look at Morennyi rock glacier indicated some relationships between velocity magnitude and surface slope. Velocity peaks generally corresponded with the crest of morphological ridges, marked by dashed lines in the elevation profile (Figure 9B). Morennyi also showed a distinct drop off in velocity upslope, with the fastest velocities observed near the terminus and central part of the landform (Figures 9A, B). Here we also saw diverging streams of flow and velocities corresponding to the surface morphology, this was prominent on the north-western side of Morennyi where we see high velocities on the diverging 'thumb' lobe. Flow direction was closely related to the local surface aspect for most rock glaciers (Table 3); Morennyi showed a particularly close relationship between vector direction and aspect (Figure 9C).

4.4 Regional analysis using open-source sentinel-2 data

The regional analysis presented feature tracking results across the 672 rock glaciers in the Northern Tien Shan (Figures 1, 10, see Supplementary Information for details). We produced flow information on many rock glaciers not covered by previous research. Rock glacier elevations ranged from 2,875 m to 4,050 m, with

TABLE 3 Velocity statistics including median, interquartile range (IQR) and mean, and results of correlation between flow and topographic characteristics for rock glacier units.

Rock glacier unit	Median velocity (m/yr)	Upper quartile (m/yr)	Mean velocity (m/yr)	Slope~velocity correlation p-value	Aspect~flow direction correlation value	Upslope connection
Timofeyeva 11A	0.65	0.90	0.56	No correlation	**0.18**	Glacier connected
Igly Tuiyksu 14B	0.64	0.79	0.62	No correlation	**0.26**	Poly-connected
RG19B	0.61	0.84	0.62	**−0.118**	**0.22**	Poly-connected
Ordzhonikidze 21A	0.53	1.91	0.92	**−0.28**	**0.35**	Glacier connected
RG4B	0.50	0.62	0.49	**−0.343**	**0.43**	Glacier connected
Igly Tuiyksu 14A	0.49	0.76	0.60	No correlation	**0.43**	Glacier forefield-connected
RG7	0.29	0.52	0.33	**0.165**	**0.17**	Talus connected
Morennyi 3	0.28	0.96	0.50	**−0.254**	**0.46**	Glacier connected
Archaly 2B	0.26	0.68	0.38	**−0.208**	**0.30**	Glacier forefield-connected
RG4C	0.25	0.36	0.25	**−0.296**	0.03	Glacier connected
RG12	0.23	0.43	0.29	**−0.039**	**0.07**	Poly-connected
Timofeyeva 11B	0.23	0.62	0.34	No correlation	**0.48**	Glacier connected
RG20	0.23	0.46	0.32	No correlation	**0.19**	Glacier forefield-connected
Gorodetsky 10A	0.22	0.31	0.21	**−0.295**	**0.20**	Glacier connected
Mayakovskiy 17	0.22	0.67	0.37	**−0.357**	**0.18**	Glacier connected
RG19A	0.22	0.31	0.24	0.048	**0.07**	Talus connected
Archaly 2C	0.17	0.27	0.20	**0.451**	**0.70**	Glacier connected
RG9	0.16	0.40	0.25	**−0.318**	**0.36**	Glacier connected
Gorodetsky 10B	0.12	0.30	0.19	**−0.242**	**0.33**	Glacier connected
Archaly 2A	0.09	0.30	0.20	**−0.424**	**0.25**	Glacier connected
RG15	0.07	0.28	0.19	**−0.294**	**0.10**	Poly-connected
RG4A	0.07	0.23	0.15	**0.196**	**0.18**	Glacier forefield-connected
RG18	0.07	0.16	0.17	No correlation	**0.14**	Poly-connected
Gorodetsky 10C	0.07	0.16	0.14	0.042	**0.17**	Glacier connected
RG16	0.06	0.08	0.12	**−0.029**	**0.24**	Poly-connected
Ordzhonikidze 21B	0.06	0.33	0.44	No correlation	**0.25**	Glacier connected
RG13	0.05	0.06	0.09	**0.093**	0.06	Glacier forefield-connected

Bold correlation results indicate statistically significant positive or negative correlations.

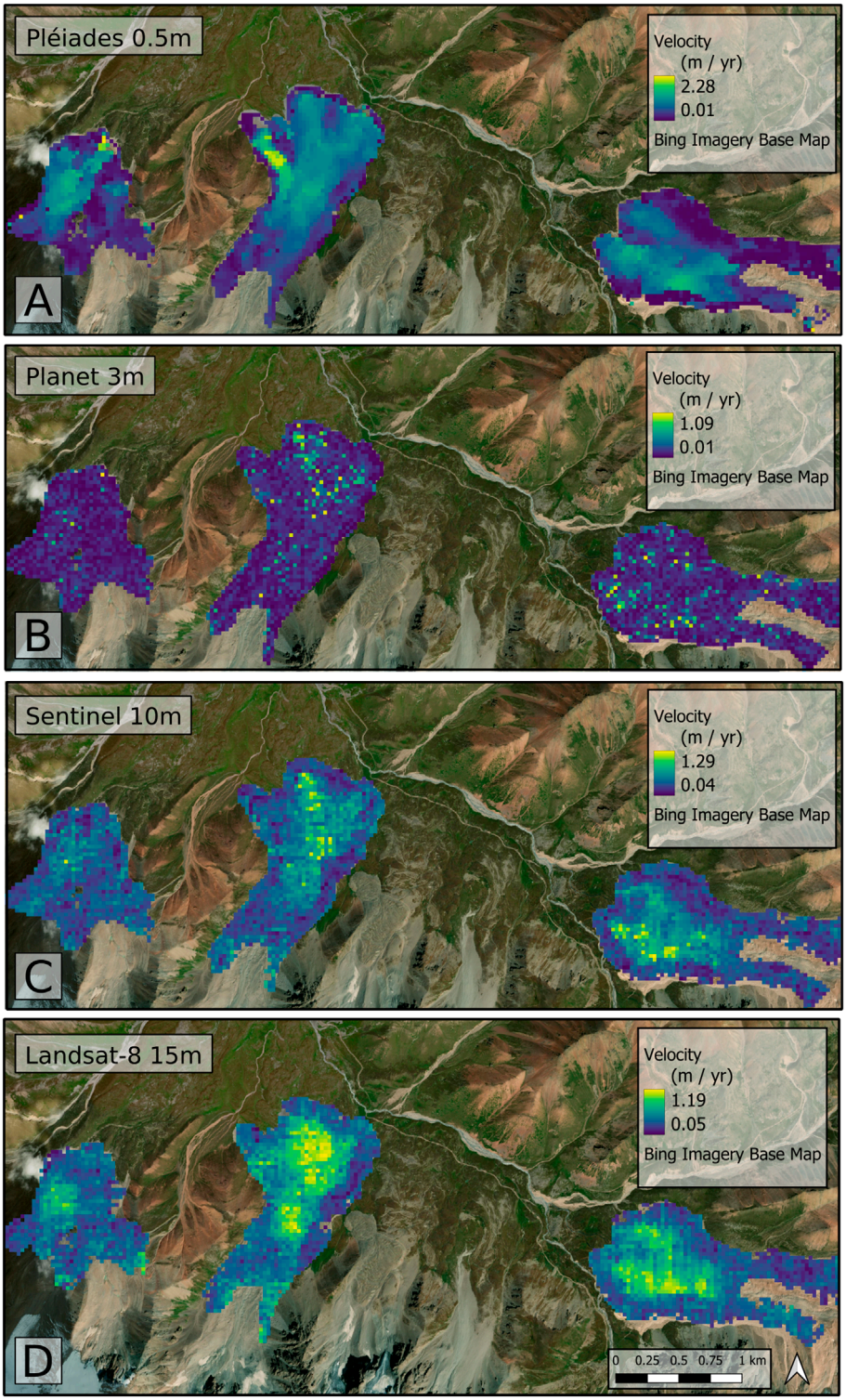

FIGURE 5
Flow velocities derived from **(A)** Pléiades (from 2016 to 2020), **(B)** Planet, **(C)** Sentinel-2 and **(D)** Landsat-8 imagery averaged per year (from 2016 to 2023) for Archaly (left), Morennyi (centre) and Gorodetsky (right) rock glaciers.

an average elevation of roughly 3,500 m. The average area was 0.30 km^2, with 25 rock glaciers exceeding 1 km^2. In terms of upslope connection, 215 rock glaciers were identified as glacier or glacier-forefield connected, 40 as poly connected and 354 as talus connected, with 63 undefined due to snow or cloud cover preventing clear identification. The mean velocity across the whole region was 0.46 m/yr with an uncertainty of 0.35 m/year. Therefore, the results on the slower moving landforms have a

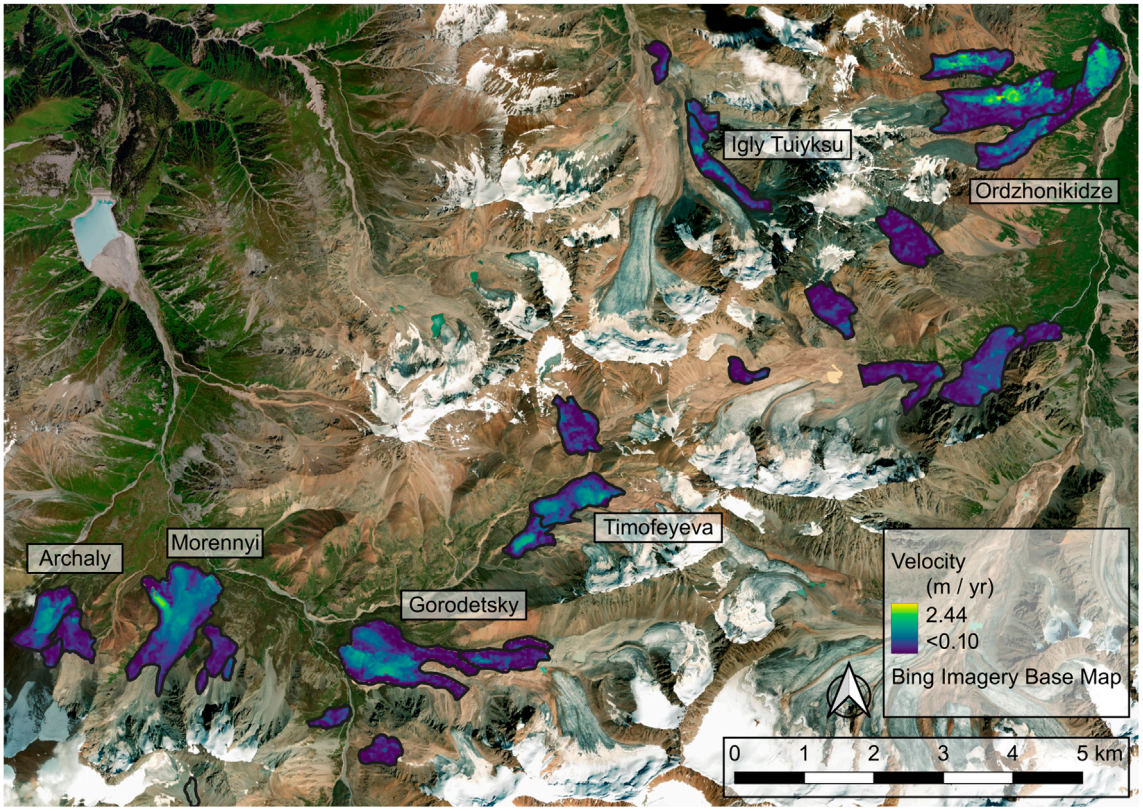

FIGURE 6
Velocity magnitude derived from analysis of high resolution Pléiades imagery collected in 2016 and 2020 for rock glaciers in the Central Ile Alatau.

high level of uncertainty, this is usually reflected by the chaotic vector fields. However, the feature tracking clearly captured active areas with high velocities on many of the rock glaciers. We found the highest velocities were exhibited on Karakorum rock glacier, Kyrgyzstan with velocities over 4 m/yr on the lower part of the rock glacier (Figure 10D). Many rock glaciers presented active areas with velocities that exceeded 2 m/yr. Considerable heterogeneity was observed within individual landforms, with distinct areas of activity and inactivity. We generally found the fastest velocities in the middle or lower part of the rock glacier (Figure 10), reflecting similar observations from the high-resolution analyses (Section 4.2). We also identified examples of upper flow lobes overriding less active lobes downslope, as seen in Figure 10, part D and E.

5 Discussion

This study looked at how optical feature tracking can be used to better understand rock glacier kinematics by examining feature tracking methods, comparing different sources of optical imagery and looking at ways of interpreting velocity results. Pléiades imagery was able to resolve complex kinematics whilst Senintel-2 and Landsat-8 data were capable of generally reproducing these patterns at a coarser resolution. The results highlighted high spatial heterogeneity in flow, with many landforms exhibiting distinct areas of high activity and relative inactivity. Rock glacier surface topography showed some relation to velocity, with faster velocities generally observed on the middle or lower slopes. Here we will discuss the results from the different scales of analysis, compare the different sensors, address the uncertainties and limitations of this study and consider the potential drivers of the patterns we observe.

5.1 Rock glacier inventory

Titkov (1988) identified 871 rock glaciers across the Northern Tien Shan based on aerial imagery; this was further refined by Gorbunov et al. (1998) who inventoried 429 rock glaciers in the Ile Alatau (former name Zailijskij Alatau). Most inventories focus on the Central Ile Alatau (Bolch and Gorbunov, 2014; Bolch and Strel, 2018; Bertone et al., 2022) and landforms in the far eastern and western extents of the mountain ranges have received considerably less research attention. This study extends the velocity inventory by Kääb et al. (2021) to include an additional 287 rock glaciers. Kääb et al. (2021) use a kinematic approach, focusing more broadly identifying slope movements from differential SAR interferograms. We chose to take a geomorphological approach and manually map the rock glacier outlines based on visible surface morphology, independent to the velocity analyses. The subjectivity of delineating rock glacier outlines is an ongoing issue as it has a significant

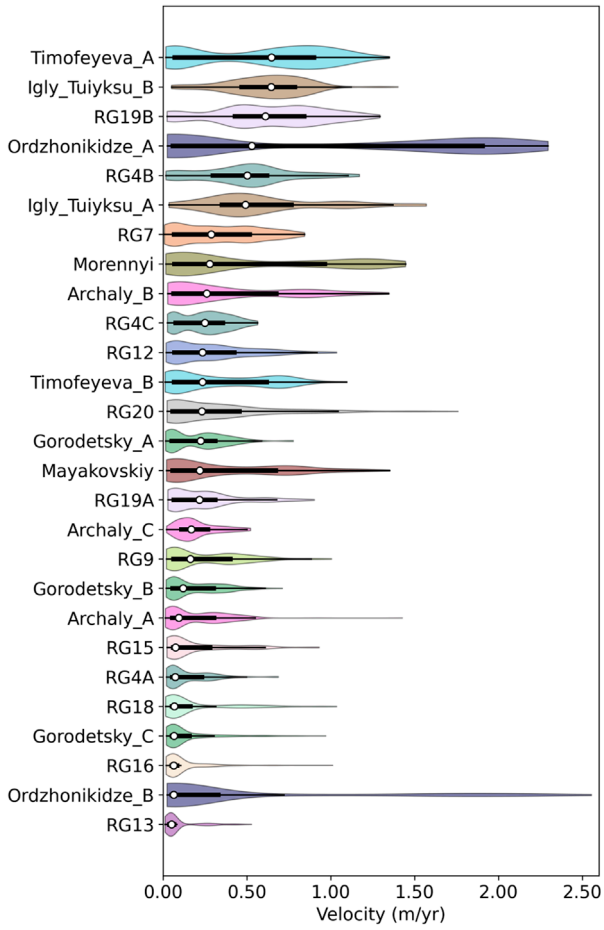

FIGURE 7
Distribution of velocity values within individual rock glacier units, indicated by width of the coloured violin body. Central black bar shows the upper and lower quartiles with the white circle indicating the median; rock glaciers are ordered by median velocity. Colours indicate rock glacier ID.

impact on both the number of rock glaciers and the extent of individual landforms. The number of rock glaciers identified by different operators has been found to vary up to a factor of 3 (Brardinoni et al., 2019). We observe evidence of this variability in rock glacier inventories for the Northern Tien Shan with the number of rock glaciers ranging from 551 (Kääb et al., 2021), to 672 (in this study) to 871 (Titkov, 1988). Rock glacier upper boundaries are also highly subjective and can differ significantly, thus limiting estimates of rock glacier surface area (Brardinoni et al., 2019). It is particularly difficult to delimitate the boundary of glacier and glacier-forefield connected rock glaciers, which are highly prevalent across the Tien Shan, from remote observations. Here we consider transitional debris covered areas with visible exposed ice and thermokarst ponds to be part of the glacier forefield and these areas have not been included in the rock glacier outlines, following suggestions from Brardinoni et al. (2019) and the RGIK (2023). The regional inventory provides new flow information, covering many rock glaciers with no previous velocity information. Whilst there are limitations to this dataset, the primary purpose of this inventory is to observe the spatial patterns of relative flow activity both between and within rock glaciers.

5.2 Comparing different sensors and scales

Previous studies applying feature tracking of satellite imagery to rock glaciers have utilised high resolution imagery, including 0.5 m resolution Geoeye, Pléiades and Worldview (Necsoiu et al., 2016; Kääb et al., 2021; Vivero et al., 2021), 2.5 m resolution Spot 5 (Necsoiu et al., 2016), and 5 m resolution RapidEye imagery (Blöthe et al., 2021). Air or UAV borne imagery is also widely used (Groh and Blothe, 2019; Cusicanqui et al., 2021) and has been used in conjunction with satellite observations (Necsoiu et al., 2016; Kääb et al., 2021; Vivero et al., 2021). However, these data are not open-source and are often limited in their spatial and temporal extent. Therefore, the potential to use open-source imagery such as Sentinel or Landsat to monitor rock glacier velocities is important for expanding the spatial and temporal coverage of kinematic information.

Our results from high-resolution Pléiades data (Figure 6) closely correspond with the feature tracking conducted by Kääb et al. (2021) on Gorodetsky, Archaly and Morennyi rock glaciers both in terms of magnitude and spatial pattern. Similar spatial patterns of flow are present across the different types of imagery, the notable exception is the result from the Planet data (Figure 5). It should be noted that the Pléiades images were acquired in 2016 and 2020 whereas the Sentinel-2, Planet and Landsat images pairs were collected in 2016 and 2023. We attribute the poor performance of the PlanetScope imagery, to the lower quality of its smallsat sensors compared to traditional satellites. The smallsat sensors exhibit significant spectral differences between individual sensors, particularly between instruments launched pre and post 2018 (Frazier and Hemingway, 2021). Issues with the spectral dynamic range (Kodl et al., 2024) and geometric distortions of PlanetScope imagery (Millan et al., 2019) are highlighted by other remote sensing research. Sentinel and Landsat data also produce better results on areas with more pronounced surface morphologies and struggle on areas with finer, loose surface material such as in the upper accumulation zone. We suggest that this may be the reason why Sentinel and Landsat don't detect the fast flow on the 'thumb' lobe of Morennyi rock glacier, as detected by the Pléiades imagery. Visual inspection of the Pléiades imagery indicates a change in the debris lithology to a smaller debris size in this section of the rock glacier.

The spatial complexity of rock glacier kinematics makes direct quantitative comparisons based on simple descriptive statistics such as the mean, maximum and minimum velocities potentially misleading (Figure 7; Table 3). For example, we interpret the very highest velocities to result from local surface movements such as small rockfalls or individual boulder displacements rather than the internal creep of the rock glacier body. The detection of these types of movements is more heavily influenced by image resolution and differences in acquisition dates so may vary between different image pairs. Furthermore, the uncertainty associated with the lower limit of detection also determines the slowest measurable velocities. Therefore, we use visual inspection and critical interpretation of the

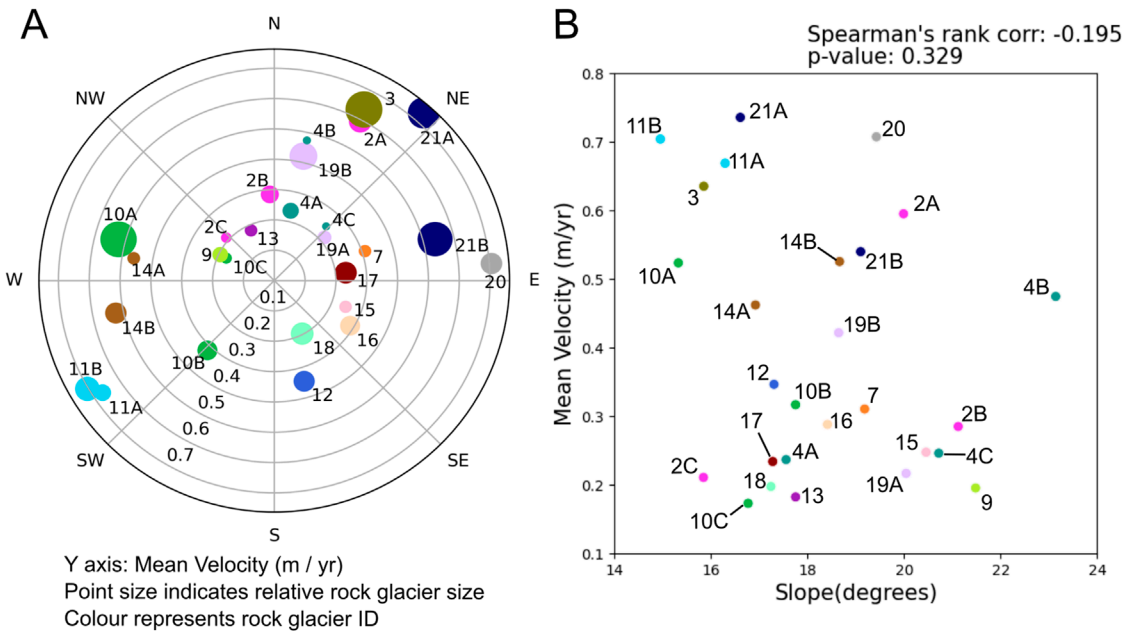

FIGURE 8
Relationships between velocity and topographic parameters (slope and aspect). **(A)** Distribution rock glacier mean aspect (circular axis) and mean velocity (*y*-axis). **(B)** Relationship between mean rock glacier velocity and mean slope angle.

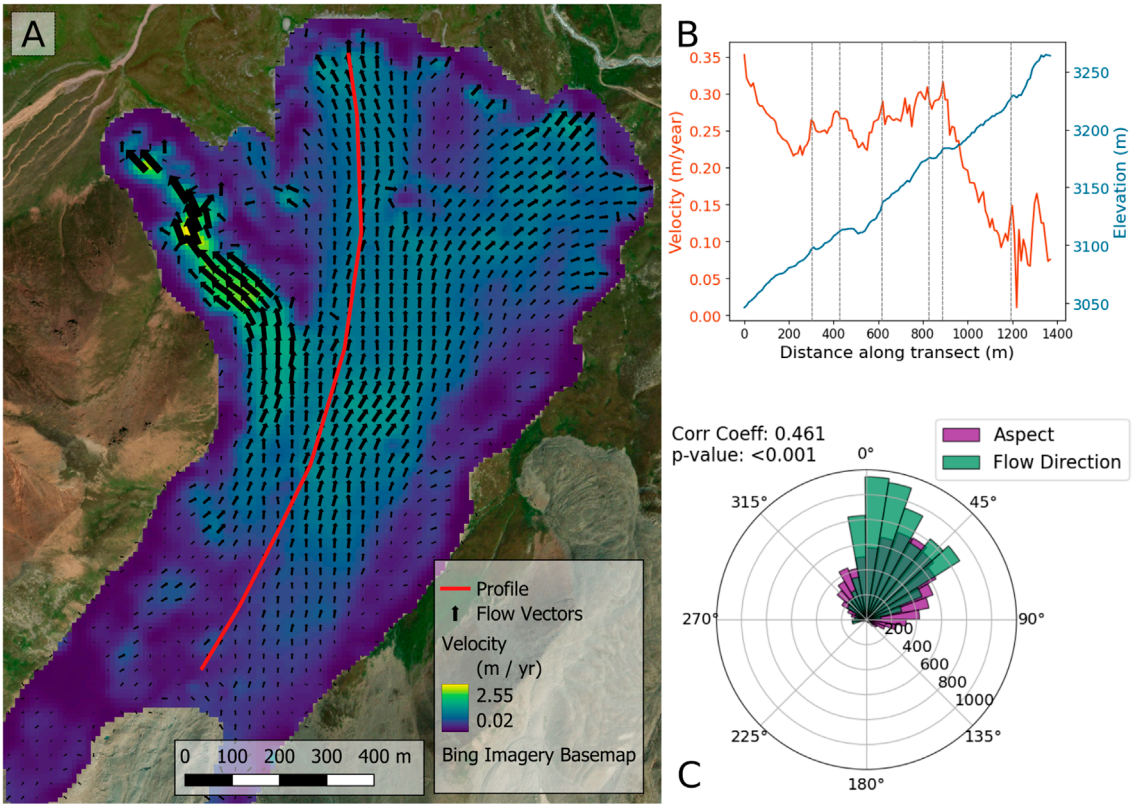

FIGURE 9
Morennyi rock glacier. **(A)** Velocity map, flow vectors scaled relative to magnitude and velocity magnitude raster. **(B)** Profile derived from transect in panel A showing velocity and elevation, dashed vertical lines indicate morphological ridges. **(C)** Rose plot of local surface aspect and flow vector direction.

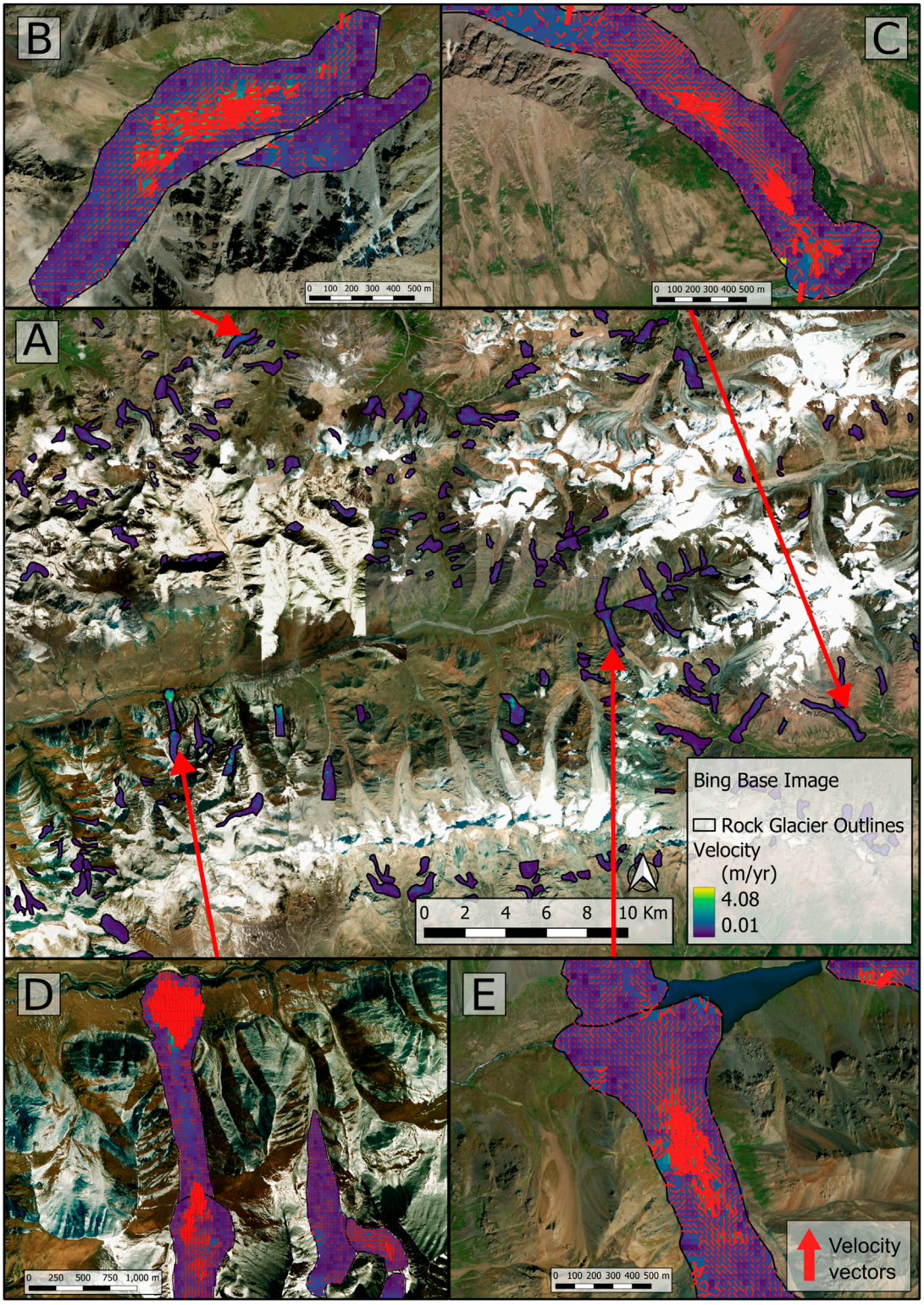

FIGURE 10
(A) Results of regional analyses of Sentinel-2 data in the central Northern Tien Shan, showing mean velocity between 2016–2023. Panel A central coordinate is 42.90N, 77.02E. Surrounding panels show results on **(B)** Burkutty **(C)** Kugalan Tash **(D)** Karakorum and **(E)** Kanbastau rock glaciers.

velocity fields as the primary means of comparison, despite its subjectivity. We suggest that for visual inspection of individual rock glaciers the flow vectors should be viewed alongside velocity magnitude. Visualising the flow vectors to show flow direction, indicates flow coherence and aids critical interpretation of the results.

5.3 Sources of error and uncertainties

Here we discuss the main sources of error, error mitigation and the uncertainties associated with our results. Errors associated with feature tracking of satellite imagery primarily arise from: offsets from image wide co-registration errors associated with the location accuracy; shifts associated with errors in the DEM used for orthorectification; feature tracking errors from inaccurate matches and the limit of detection (Kääb et al., 2016; Kääb et al., 2021). Whilst we cannot completely remove these signals, we improve the feature tracking results through pre and post processing. Initial co-registration reduces the error associated with location accuracy (Scheffler et al., 2017). However, steep slopes and mountainous terrain produce localised distortions and non-linear co-registration errors not corrected for by simple XY shifts, often arising from vertical errors with the DEM used for the original image orthorectification. These types of errors are difficult to quantify as they are spatially variable (Kääb et al., 2021), whilst we acknowledge them here we are not able to explicitly correct for them. A localised co-registration method using Arosics was considered by this study, however, the potential bias introduced by this was deemed to be a greater source of uncertainty. The post processing aims to remove erroneous matches from the feature tracking by applying a series of filters to remove obvious outliers. We do this using neighbourhood filters that compare each pixel to the mean of its surrounding pixels. The directional neighbourhood filter was set to 90°, as a lower 30° filter as used by Kääb et al. (2021) was found to remove valid data points in areas of diverging flow. At the regional scale, greater variability in flow characteristics make it more difficult to target the post-processing filters, so the number of remaining erroneous vectors is higher. For the smaller and slower moving rock glaciers the rate of flow may be below the uncertainty threshold, and this is usually also reflected in an incoherent flow field.

The limit of detection of the feature tracking algorithm is a source of uncertainty associated with the resolution of the input imagery. Scheffler et al. (2017) suggest that Arosics can detect displacements at a sub-pixel resolution of 1/3 of a pixel or greater. We consider the limit of detection to be the greatest source of uncertainty we are not able to correct for, so have used this to characterise overall uncertainty. We take the mean displacement on areas of stable ground to be the lower limit of detection, making the uncertainty 0.21 m/yr for Pléiades and 0.35 m/year for Sentinel (Table 2). The mean offset on stable ground for the Planet imagery is 0.15 m/yr however, we attribute this lower value largely due to the feature tracking failing to detect matches on many points. Measures of variance are used to characterise feature tracking uncertainty by previous studies (Kääb et al., 2021; Villarroel et al., 2018). However, after calculating the standard deviation of stable ground offsets, the limit of detection remains a greater uncertainty for all sources of imagery (Table 2).

5.4 Drivers of heterogeneity

Comparison between mean surface velocity, area and aspect shows large fast flowing rock glaciers are more prevalent for North Easterly or South Westerly/Westerly orientations (Figure 8B). This reflects the overall orientation of the mountain range running South East–North West, suggesting valley orientation is a controlling factor in determining where large, faster flowing rock glaciers can form.

A compressional flow regime is traditionally considered responsible for the characteristic ridge and furrow topography of rock glaciers (Wahrhaftig and Cox, 1959; Kääb and Weber, 2004). This compression results from faster flow upslope that decreases in the mid to lower rock glacier. An example of this spatial pattern can be observed on the Dos Lenguas rock glacier in Argentina (Halla et al., 2021). However, our results generally observe the fastest velocities on the lower rock glacier, near to the front. This is supported by the negative relationship between slope and velocity magnitude exhibited by many rock glaciers (Table 3) and visible observations from both the high-resolution velocity data (Figures 6, 9) and the regional scale analysis (Figure 10). This pattern of velocities increasing downslope, with the fastest velocities near the front, suggests an extensional flow regime. Furthermore, we see a lack of evidence of significant material input in the accumulation zone as might be expected. Similar interpretations were made by Krainer and Mostler (2006) and Hausmann et al. (2012) for Ölgrube rock glacier in Austria. Whilst our results don't suggest current rock glacier-wide compressional flow, the rock glaciers do exhibit ridge and furrow topography indicating past compressional flow, and we do see examples of faster flowing upper lobes overriding less active lobes below (Figure 10). This region is experiencing climate changes; data from Tuyuksu Glacier weather station in Kazakhstan shows a significant trend of rising September temperatures but with variable precipitation (see Supplementary Information).

This leads us to interpret that flow spatial heterogeneity may be driven by differences in internal structure and ice content, as a result of historical conditions. Ice content determines the rheological properties of the rock glacier, which is a major control on flow processes (Hu et al., 2023). Previous work suggests that rock glacier characteristics in this region may be closely linked to glacier interactions, intensive weathering and avalanche events (Bolch and Gorbunov, 2014). Geophysical investigations on two rock glaciers in the Central Tien Shan by Bolch et al. (2019) indicate the presence of debris-covered ice existing under permafrost conditions, likely deposited by past glacier advances or surges. Mathys et al. (2024) report that rock glaciers in the Pamir and Kyrgyz Tien Shan exhibit variable ice contents of 38%–60%. They also observe significant heterogeneity in the ice content and distribution of ice within glacial moraines and identify a body of pure ice in the Abramov rock glacier, which they interpret as being of glacial origin. These findings suggest the potential for heterogeneous incorporation of glacial ice into glacier or glacier-forefield connected rock glaciers. Similar findings are observed on the Gruben rock glacier in the Swiss Alps, where surface elevation changes and velocities are linked to historical fluctuations in the polythermal Gruben glacier (Kääb et al., 1997). The connection of many rock glaciers in the Northern Tien Shan to glaciers and glacier forefields, indicates that some rock glaciers could contain depositions of glacier ice preserved under permafrost conditions. We expect this to be reflected in their surface flow processes. This provides a strong rationale for the cause of the spatial heterogeneity in surface flow we observe today.

Rock glaciers in the Tien Shan are an interconnected part of the glacial and periglacial environment and play an important hydrologic and geomorphic role in the landscape's deglaciation. These rock glaciers are likely to contain significant quantities of ice,

particularly within the larger ice-debris complexes, which tend to be glacier or glacier forefield connected. The response of rock glaciers and ice-debris landforms to climate changes will differ from that of glaciers. This has implications for understanding ice storage and glacier water resources. There is a need for more field data on their internal structure and composition (through geophysical surveys or boreholes) as current measurements are limited in Central Asia (Bolch et al., 2019; Mathys et al., 2024).

6 Conclusion

This study implemented a new feature tracking processing workflow using frequency domain cross-correlation for deriving velocities on rock glaciers. The method was tested on Pléiades, Planet, Sentinel-2 and Landsat-8 data. Comparison of the different sources of imagery showed Sentinel-2 data to be capable of reproducing patterns of flow detected from high-resolution imagery. Planet data performed comparatively poorly, likely due to limitations with the spectral dynamic range of the Planet sensors.

Analysis of high-resolution Pléiades imagery in the Central Ile Alatau revealed high spatial variability. The fastest median velocities of 0.65 m/yr (upper quartile 0.90 m/yr) were observed on Timofeyeva rock glacier. High levels of activity were also exhibited on Ordzhonikidze (median velocity 0.53 m/yr, upper quartile 1.91 m/yr) and Morennyi (median velocity 0.28 m/yr, upper quartile 0.96 m/yr), however, these rock glaciers exhibited more heterogenous velocity distributions. Several of the rock glaciers exhibited bimodal velocity distributions with distinct areas of high activity and relative inactivity. This demonstrates the limitations of using single mean or median statistics to represent overall rock glacier flow.

Regional analyses using Sentinel-2 data extended existing velocity inventories to cover 672 rock glaciers across the Northern Tien Shan. Both the high-resolution and regional scale analyses generally found the highest velocities on the middle or lower slopes near the rock glacier front. Our findings suggested that the spatial heterogeneity exhibited by many rock glaciers, particularly on glacier or glacier-forefield connected landforms is linked to historic environmental fluctuations. To better understand this there is a need for more information on rock glacier internal structure through boreholes or geophysical investigations.

Data availability statement

The datasets presented in this study can be found in online repositories. The names of the repository/repositories and accession number(s) can be found in the article/Supplementary Material.

Author contributions

EW: Conceptualization, Data curation, Formal Analysis, Investigation, Methodology, Project administration, Validation, Visualization, Writing–original draft, Writing–review and editing. TB: Conceptualization, Funding acquisition, Resources, Supervision, Writing–review and editing. RS: Project administration, Resources, Supervision, Writing–review and editing.

Funding

The author(s) declare that financial support was received for the research, authorship, and/or publication of this article. EW was funded by the Global Doctoral Scholarship between the University of St Andrews and the University of Bonn. The work by TB was supported by the Kazakhstan Program of Targeted Financing of Scientific Research, "Glacial systems of Central Asia transboundary basins: condition, current and forecast changes, role in ensuring water security of region countries," grant number BR18574176. Publication fees were supported by St Andrews open access fund.

Acknowledgments

We acknowledge the support Lothar Schrott for his guidance and thank him and Francesca Baldacchino for their feedback on the paper. We are also grateful for the support of the Central-Asian regional glaciological centre of category 2 under the auspices of UNESCO (I. Severskiy, V. Kapitsa, A. Yegorov) for providing guidance on the rock glacier names, knowledge of the study area and climate data from the Tuyuksu weather station. We acknowledge CNES and Airbus Defence and Space for the provision of the Pléiades data at a reduced cost though the ISIS project (© CNES and Airbus DS, 2016, 2020, all rights reserved).

Conflict of interest

The authors declare that the research was conducted in the absence of any commercial or financial relationships that could be construed as a potential conflict of interest.

Generative AI statement

The author(s) declare that no Generative AI was used in the creation of this manuscript.

Publisher's note

Supplementary material

The Supplementary Material for this article can be found online at: https://www.frontiersin.org/articles/10.3389/feart.2024.1518390/full#supplementary-material

References

Azócar, G., and Brenning, A. (2010). Hydrological and geomorphological significance of rock glaciers in the Dry Andes, Chile (27°-33°S). *Permafr. Periglac. Process.* 21, 42–53. doi:10.1002/ppp.669

Barboux, C., Delaloye, R., and Lambiel, C. (2014). Inventorying slope movements in an Alpine environment using DInSAR. *Earth Surf. Process. Landf.* 39, 2087–2099. doi:10.1002/esp.3603

Barsch, D., and Jakob, M. (1998). Mass transport by active rockglaciers in the Khumbu Himalaya. *GEOMORPHOLOGY* 26, 215–222. doi:10.1016/S0169-555X(98)00060-9

Berthling, I. (2011). Beyond confusion: rock glaciers as cryo-conditioned landforms. *Geomorphology* 131, 98–106. doi:10.1016/j.geomorph.2011.05.002

Bertone, A., Barboux, C., Bodin, X., Bolch, T., Brardinoni, F., Caduff, R., et al. (2022). Incorporating InSAR kinematics into rock glacier inventories: insights from 11 regions worldwide. *Cryosphere* 16, 2769–2792. doi:10.5194/tc-16-2769-2022

Bhattacharya, A., Bolch, T., Mukherjee, K., King, O., Menounos, B., Kapitsa, V., et al. (2021). High Mountain Asian glacier response to climate revealed by multi-temporal satellite observations since the 1960s. *Nat. Commun.* 12, 4133. doi:10.1038/s41467-021-24180-y

Blothe, J. H., Halla, C., Schwalbe, E., Bottegal, E., Liaudat, D. T., and Schrott, L. (2021). Surface velocity fields of active rock glaciers and ice-debris complexes in the Central Andes of Argentina. *Earth Surf. Process. Landf.* 46, 504–522. doi:10.1002/esp.5042

Blothe, J. H., Rosenwinkel, S., Hoser, T., and Korup, O. (2019). Rock-glacier dams in high Asia. *Earth Surf. Process. Landf.* 44, 808–824. doi:10.1002/esp.4532

Bolch, T. (2007). Climate change and glacier retreat in northern Tien Shan (Kazakhstan/Kyrgyzstan) using remote sensing data. *Glob. Planet. Change* 56, 1–12. doi:10.1016/j.gloplacha.2006.07.009

Bolch, T. (2017). Asian glaciers are a reliable water source. *Nature* 545, 161–162. doi:10.1038/545161a

Bolch, T., and Gorbunov, A. P. (2014). Characteristics and origin of rock glaciers in northern tien Shan (Kazakhstan/Kyrgyzstan). *Permafr. Periglac. Process.* 25, 320–332. doi:10.1002/ppp.1825

Bolch, T., and Marchenko, S. (2009). Significance of glaciers, rockglaciers and ice-rich permafrost in the Northern Tien Shan as water towers under climate change conditions. *Present. A. T. Assess. Snow, Glacier Water Resour. Asia, IHP/HWRP-Berichte, Almaty, Kazakhstan*, 132–144.

Bolch, T., Rohrbach, N., Kutuzov, S., Robson, B. A., and Osmonov, A. (2019). Occurrence, evolution and ice content of ice-debris complexes in the Ak-Shiirak, Central Tien Shan revealed by geophysical and remotely-sensed investigations. *Earth Surf. Process. Landf.* 44, 129–143. doi:10.1002/esp.4487

Bolch, T., and Strel, A. (2018). "Evolution of rock glaciers in northern Tien Shan," in Presented at the 5th European Conference on Permafrost, Laboratoire EDYTEM, Chamonix, Chamonix, 1 July 2018, 48–49.

Brardinoni, F., Scotti, R., Sailer, R., and Mair, V. (2019). Evaluating sources of uncertainty and variability in rock glacier inventories. *Earth Surf. Process. Landf.* 44, 2450–2466. doi:10.1002/esp.4674

Chen, Y. N., Li, W. H., Deng, H. J., Fang, G. H., and Li, Z. (2016). Changes in central asia's water tower: past, present and future. *Sci. Rep.* 6, 35458. doi:10.1038/srep39364

Cusicanqui, D., Rabatel, A., Vincent, C., Bodin, X., Thibert, E., and Francou, B. (2021). Interpretation of volume and flux changes of the laurichard Rock Glacier between 1952 and 2019, French Alps. *J. Geophys. Res.-Earth Surf.* 126. doi:10.1029/2021JF006161

Dehecq, A., Gourmelen, N., Gardner, A. S., Brun, F., Goldberg, D., Nienow, P. W., et al. (2019). Twenty-first century glacier slowdown driven by mass loss in High Mountain Asia. *Nat. Geosci.* 12, 22–27. doi:10.1038/s41561-018-0271-9

Delaloye, R., Lambiel, C., and Gartner-Roer, I. (2010). Overview of rock glacier kinematics research in the Swiss Alps: seasonal rhythm, interannual variations and trends over several decades. *Geogr. Helvetica* 65, 135–145. doi:10.5194/gh-65-135-2010

Farinotti, D., Longuevergne, L., Moholdt, G., Duethmann, D., Molg, T., Bolch, T., et al. (2015). Substantial glacier mass loss in the Tien Shan over the past 50 years. *Nat. Geosci.* 8, 716–722. doi:10.1038/Ngeo2513

Frazier, A. E., and Hemingway, B. L. (2021). A technical review of Planet smallsat data: practical considerations for processing and using PlanetScope imagery. *Remote Sens.* 13, 3930. doi:10.3390/rs13193930

Gorbunov, A., Severskiy, E., Titkov, S., Marchenko, S., and Popov, M. (1998). Rock glaciers, zailiysiky range, kungei ranges. *Tienshan, Kazakhstan*. Boulder, CO. National Snow and Ice Data Center. (GGDSOI,Version 1). doi:10.7265/51zk-r767

Gorbunov, A., and Titkov, S. (1989). *Kamennye gletchery gor srednej azii: (rock glaciers of the central asian mountains)*. Irkutsk: Akad. Nauk SSSR.

Gorbunov, A. P., Titkov, S. N., and Polyakov, V. G. (1992). Dynamics of rock glaciers of the northern tien Shan and the djungar Ala tau, Kazakhstan. *Permafr. Periglac. Process.* 3, 29–39. doi:10.1002/ppp.3430030105

Groh, T., and Blothe, J. H. (2019). Rock Glacier kinematics in the kaunertal, otztal Alps, Austria. *Geosciences* 9, 373. doi:10.3390/geosciences9090373

Gruen, A. (2012). Development and status of image matching in photogrammetry. *Photogramm. Rec.* 26, 36–57. doi:10.1111/j.1477-9730.2011.00671.x

Halla, C., Blöthe, J. H., Tapia Baldis, C., Trombotto Liaudat, D., Hilbich, C., Hauck, C., et al. (2021). Ice content and interannual water storage changes of an active rock glacier in the dry Andes of Argentina. *Cryosphere* 15, 1187–1213. doi:10.5194/tc-15-1187-2021

Hassan, J., Chen, X. Q., Muhammad, S., and Bazai, N. A. (2021). Rock glacier inventory, permafrost probability distribution modeling and associated hazards in the Hunza River Basin, Western Karakoram, Pakistan. *Sci. Total Environ.* 782, 146833. doi:10.1016/j.scitotenv.2021.146833

Hausmann, H., Krainer, K., Brückl, E., and Ullrich, C. (2012). Internal structure, ice content and dynamics of Ölgrube and Kaiserberg rock glaciers (Ötztal Alps, Austria) de-termined from geophysical surveys. Austrian J. *Earth Sci.* 105, 12–31.

Havenith, H. B., Strom, A., Torgoev, I., Torgoev, A., Lamair, L., Ischuk, A., et al. (2015). Tien Shan geohazards database: earthquakes and landslides. *Applications* 249, 16–31. doi:10.1016/j.geomorph.2015.01.037

Heid, T., and Kaab, A. (2012). Evaluation of existing image matching methods for deriving glacier surface displacements globally from optical satellite imagery. *Remote Sens. Environ.* 118, 339–355. doi:10.1016/j.rse.2011.11.024

Hu, Y., Harrison, S., Liu, L., and Wood, J. L. (2023). Modelling rock glacier ice content based on InSAR-derived velocity, Khumbu and Lhotse valleys, Nepal. *Cryosphere* 17, 2305–2321. doi:10.5194/tc-17-2305-2023

Immerzeel, W. W., and Bierkens, M. F. P. (2012). Asia's water balance. *Nat. Geosci.* 5, 841–842. doi:10.1038/ngeo1643

Janke, J. R., and Bolch, T. (2021). "Rock glaciers," in *Treatise on geomorphology*. Editor H. Haritashya (Elsevier).

Jones, D. B., Harrison, S., and Anderson, K. (2019). Mountain glacier-to-rock glacier transition. *Glob. Planet. Change* 181, 102999. doi:10.1016/j.gloplacha.2019.102999

Jones, D. B., Harrison, S., Anderson, K., Shannon, S., and Betts, R. A. (2021). Rock glaciers represent hidden water stores in the Himalaya. *Sci. Total Environ.* 793, 145368. doi:10.1016/j.scitotenv.2021.145368

Kääb, A., Frauenfelder, R., and Roer, I. (2007). On the response of rockglacier creep to surface temperature increase. *Glob. Planet. Change* 56, 172–187. doi:10.1016/j.gloplacha.2006.07.005

Kääb, A., Haeberli, W., and Gudmundsson, G. H. (1997). Analysing the creep of mountain permafrost using high precision aerial photogrammetry: 25 years of monitoring Gruben rock glacier, Swiss Alps. *Permafr. Periglac. Process.* 8, 409–426. doi:10.1002/(SICI)1099-1530(199710/12)8:4<409::AID-PPP267>3.0.CO;2-C

Kääb, A., and Røste, J. (2024). Rock glaciers across the United States predominantly accelerate coincident with rise in air temperatures. *Nat. Commun.* 15, 7581. doi:10.1038/s41467-024-52093-z

Kääb, A., Strozzi, T., Bolch, T., Caduff, R., Trefall, H., Stoffel, M., et al. (2021). Inventory and changes of rock glacier creep speeds in Ile Alatau and Kungoy Ala-Too, northern Tien Shan, since the 1950s. *Cryosphere* 15, 927–949. doi:10.5194/tc-15-927-2021

Kääb, A., and Vollmer, M. (2000). Surface geometry, thickness changes and flow fields on creeping mountain permafrost: automatic extraction by digital image analysis. *Permafr. Periglac. Process.* 11, 315–326. doi:10.1002/1099-1530(200012)11:4<315::Aid-Ppp365>3.0.Co;2-J

Kääb, A., and Weber, M. (2004). Development of transverse ridges on rock glaciers: field measurements and laboratory experiments. *Permafr. Periglac. Process.* 15, 379–391. doi:10.1002/ppp.506

Kääb, A., Winsvold, S. H., Altena, B., Nuth, C., Nagler, T., and Wuite, J. (2016). Glacier remote sensing using sentinel-2. Part I: radiometric and geometric performance, and application to ice velocity. *Remote Sens.* 8, 598. doi:10.3390/rs8070598

Kaldybayev, A., Sydyk, N., Yelisseyeva, A., Merekeyev, A., Nurakynov, S., Zulpykharov, K., et al. (2023). The first inventory of rock glaciers in the zhetysu Alatau: the aksu and lepsy river basins. *Remote Sens.* 15, 197. doi:10.3390/rs15010197

Kellerer-Pirklbauer, A., Bodin, X., Delaloye, R., Lambiel, C., Gärtner-Roer, I., Bonnefoy-Demongeot, M., et al. (2024). Acceleration and interannual variability of creep rates in mountain permafrost landforms (rock glacier velocities) in the European Alps in 1995 2022. *Environ. Res. Lett.* 19, 034022. doi:10.1088/1748-9326/ad25a4

Kellerer-Pirklbauer, A., Lieb, G. K., and Kaufmann, V. (2017). The Dösen Rock Glacier in Central Austria: a key site for multidisciplinary long-term rock glacier monitoring in the Eastern Alps. *Earth Sci.* 110. doi:10.17738/ajes.2017.0013

Kodl, G., Streeter, R., Cutler, N., and Bolch, T. (2024). Arctic tundra shrubification can obscure increasing levels of soil erosion in NDVI assessments of land cover derived from satellite imagery. *Remote Sens. Environ.* 301, 113935. doi:10.1016/j.rse.2023.113935

Krainer, K., and Mostler, W. (2006). Flow velocities of active rock glaciers in the Austrian Alps. *Geogr. Ann. Ser. Phys. Geogr.* 88, 267–280. doi:10.1111/j.0435-3676.2006.00300.x

Lilleoren, K. S., Etzelmuller, B., Gartner-Roer, I., Kaab, A., Westermann, S., and Gudmundsson, A. (2013). The distribution, thermal characteristics and dynamics of permafrost in trollaskagi, northern Iceland, as inferred from the distribution of rock glaciers and ice-cored moraines. *Permafr. Periglac. Process.* 24, 322–335. doi:10.1002/ppp.1792

Liu, L., Millar, C. I., Westfall, R. D., and Zebker, H. A. (2013). Surface motion of active rock glaciers in the Sierra Nevada, California, USA: inventory and a case study using InSAR. *Cryosphere* 7, 1109–1119. doi:10.5194/tc-7-1109-2013

Marcer, M., Cicoira, A., Cusicanqui, D., Bodin, X., Echelard, T., Obregon, R., et al. (2021). Rock glaciers throughout the French Alps accelerated and destabilised since 1990 as air temperatures increased. *Commun. Earth Environ.* 2, 81. doi:10.1038/s43247-021-00150-6

Mathys, T., Azimshoev, M., Bektursunov, Z., Hauck, C., Hilbich, C., Duishonakunov, M., et al. (2024). Quantifying permafrost ground ice contents in the tien Shan and Pamir (central Asia): a petrophysical joint inversion approach using the geometric mean model. *EGUsphere*, 1–52. doi:10.5194/egusphere-2024-2795

Millan, R., Mouginot, J., Rabatel, A., Jeong, S., Cusicanqui, D., Derkacheva, A., et al. (2019). Mapping surface flow velocity of glaciers at regional scale using a multiple sensors approach. *Remote Sens.* 11, 2498. doi:10.3390/rs11212498

Millan, R., Mouginot, J., Rabatel, A., and Morlighem, M. (2022). Ice velocity and thickness of the world's glaciers. *Nat. Geosci.* 15, 124–129. doi:10.1038/s41561-021-00885-z

Monnier, S., and Kinnard, C. (2017). Pluri-decadal (1955–2014) evolution of glacier–rock glacier transitional landforms in the central Andes of Chile (30–33° S). *Earth Surf. Dyn.* 5, 493–509. doi:10.5194/esurf-5-493-2017

Necsoiu, M., Onaca, A., Wigginton, S., and Urdea, P. (2016). Rock glacier dynamics in Southern Carpathian Mountains from high-resolution optical and multi-temporal SAR satellite imagery. *Remote Sens. Environ.* 177, 21–36. doi:10.1016/j.rse.2016.02.025

Niederer, P., Bilenko, V., Ershova, N., Hurni, H., Yerokhin, S., and Maselli, D. (2008). Tracing glacier wastage in the Northern Tien Shan (Kyrgyzstan/Central Asia) over the last 40 years. *Clim. Change* 86, 227–234. doi:10.1007/s10584-007-9288-6

Pieczonka, T., and Bolch, T. (2015). Region-wide glacier mass budgets and area changes for the Central Tien Shan between ~1975 and 1999 using Hexagon KH-9 imagery. *Glob. Planet. Change* 128, 1–13. doi:10.1016/j.gloplacha.2014.11.014

RGIK (2023). Guidelines for inventorying rock glaciers: baseline and practical concepts (Version 1.0). *IPA Action Group Rock glacier Invent. Kinemat.* doi:10.51363/unifr.srr.2023.002

Scambos, T. A., Dutkiewicz, M. J., Wilson, J. C., and Bindschadler, R. A. (1992). Application of image cross-correlation to the measurement of glacier velocity using satellite image data. *Remote Sens. Environ.* 42, 177–186. doi:10.1016/0034-4257(92)90101-O

Scheffler, D., Hollstein, A., Diedrich, H., Segl, K., and Hostert, P. (2017). AROSICS: an automated and robust open-source image Co-registration software for multi-sensor satellite data. *Remote Sens.* 9, 676. doi:10.3390/rs9070676

Schrott, L. (1996). Some geomorphological-hydrological aspects of rock glaciers in the Andes (San Juan, Argentina). *Z. Geomorphol. Suppl.* 104, 161–173.

Shahgedanova, M., Afzal, M., Hagg, W., Kapitsa, V., Kasatkin, N., Mayr, E., et al. (2020). Emptying water towers? Impacts of future climate and glacier change on river discharge in the northern tien Shan, central Asia. *Water* 12, 627. doi:10.3390/w12030627

Shahgedanova, M., Afzal, M., Severskiy, I., Usmanova, Z., Saidaliyeva, Z., Kapitsa, V., et al. (2018). Changes in the mountain river discharge in the northern Tien Shan since the mid-20th Century: results from the analysis of a homogeneous daily streamflow data set from seven catchments. *J. Hydrol.* 564, 1133–1152. doi:10.1016/j.jhydrol.2018.08.001

Sorg, A., Bolch, T., Stoffel, M., Solomina, O., and Beniston, M. (2012). Climate change impacts on glaciers and runoff in Tien Shan (Central Asia). *Nat. Clim. Change* 2, 725–731. doi:10.1038/Nclimate1592

Sorg, A., Kaab, A., Roesch, A., Bigler, C., and Stoffel, M. (2015). Contrasting responses of Central Asian rock glaciers to global warming. *Sci. Rep.* 5, 8228. doi:10.1038/srep08228

Strozzi, T., Caduff, R., Jones, N., Barboux, C., Delaloye, R., Bodin, X., et al. (2020). Monitoring Rock Glacier kinematics with satellite synthetic aperture radar. *Remote Sens.* 12, 559. doi:10.3390/rs12030559

Strozzi, T., Kaab, A., and Frauenfelder, R. (2004). Detecting and quantifying mountain permafrost creep from *in situ* inventory, space-borne radar interferometry and airborne digital photogrammetry. *Int. J. Remote Sens.* 25, 2919–2931. doi:10.1080/0143116042000192330

Thibert, E., and Bodin, X. (2022). Changes in surface velocities over four decades on the Laurichard rock glacier (French Alps). *Permafr. Periglac. Process.* 33, 323–335. doi:10.1002/ppp.2159

Titkov, S. N. (1988). *Rock glaciers and glaciation of the central Asia mountains*. Tapir Publ.

Villarroel, C. D., Beliveau, G. T., Forte, A. P., Monserrat, O., and Morvillo, M. (2018). DInSAR for a regional inventory of active rock glaciers in the dry andes mountains of Argentina and Chile with sentinel-1 data. *Remote Sens.* 10, 1588. doi:10.3390/rs10101588

Vivero, S., Bodin, X., Farías-Barahona, D., MacDonell, S., Schaffer, N., Robson, B. A., et al. (2021). Combination of aerial, satellite, and UAV photogrammetry for quantifying Rock Glacier kinematics in the dry andes of Chile (30°S) since the 1950s. *Front. Remote Sens.* 2. doi:10.3389/frsen.2021.784015

Wahrhaftig, C., and Cox, A. (1959). Rock glaciers in the Alaska range. *BullGeolSoc Am.* 70, 383–436. doi:10.1130/0016-7606(1959)70[383:rgitar]2.0.co;2

Wang, X. W., Liu, L., Zhao, L., Wu, T. H., Li, Z. Q., and Liu, G. X. (2017). Mapping and inventorying active rock glaciers in the northern Tien Shan of China using satellite SAR interferometry. *Cryosphere* 11, 997–1014. doi:10.5194/tc-11-997-2017

Wirz, V., Gruber, S., Purves, R. S., Beutel, J., Gartner-Roer, I., Gubler, S., et al. (2016). Short-term velocity variations at three rock glaciers and their relationship with meteorological conditions. *Earth Surf. Dyn.* 4, 103–123. doi:10.5194/esurf-4-103-2016

Yadav, R. R., and Kulieshius, P. (1992). Dating of earthquakes: tree ring responses to the catastrophic earthquake of 1887 in alma-ata, Kazakhstan. *Geogr. J.* 158, 295–299. doi:10.2307/3060298

Zhang, Q. F., Chen, Y. N., Li, Z., Xiang, Y. Y., Li, Y. P., and Sun, C. J. (2022). Recent changes in glaciers in the northern tien Shan, central Asia. *Remote Sens.* 14, 2878. doi:10.3390/rs14122878